PAPER NUMBER

532

CORROSION 90

April 23-27, 1990 · Bally's Hotel, Las Vegas, Nevada

MICROBIOLOGICALLY INFLUENCED CORROSION OF 6% MOLYBDENUM STAINLESS STEELS and AISI 316: COMPARISON WITH FERRIC CHLORIDE TESTING.

N.J.E. Dowling, D.C. White, R.A. Buchanan, J.C. Danko, A. Vass, and S.Brooks.
Institute for Applied Microbiology, Blg. 1, Suite 300, 10515 Research Drive, Knoxville, TN. 37932.

Gary L. Ward
Duke Power Co., Nuclear Production Dept., P.O. Box 33189, 422 S.Church St., Charlotte, NC 28242.

ABSTRACT

Three stainless steel alloys were exposed to selected bacteria in a low conductivity test system. Two of the alloys contained 6% molybdenum as compared to one with 2.5%. The corrosion rates and open circuit potentials indicated that after approximately 30 hours exposure an alloy with 6% Mo and 24% Ni had the highest corrosion rate at that time. Subsequent corrosion analysis of the same coupons under ferric chloride attack (after ASTM G48-76) demonstrated that the "chemical" corrosion characteristics and ranking were different from that observed under microbially influenced corrosion attack (MIC). This data therefore indicates that resistance to ferric chloride testing may not necessarily imply similar resistance to MIC.

INTRODUCTION

The microbially influenced corrosion (MIC) of stainless steels is a well established process (1,2,3) that is little understood. Stainless steels are alloys that possess exceptional corrosion characteristics due to the rapid formation of a passive surface film (4). This film has been described by Okamoto (5) and appears to consist of a crystalline oxy-hydroxide lattice where the stability is provided by surface enriched chromium and nickel. While this film's remarkable properties usually allow quick repair,

the sorbtion of anions such as chloride and sulfate (6) promote pitting and localized dissolution. To mitigate this effect in high chloride environments molybdenum is added (4) for example. In AISI 316 the addition of approximately 2.5% Mo significantly improves the pitting resistance. More recently the development of the so-called "super-austenitic" stainless steels have increased the molybdenum content to approximately 6% and nitrogen to 0.1 to 0.2 %. These alloys are considered to be exceptional in highly corrosive chloride-containing environments.

Current methods to assess the pitting resistance of such alloys include the ferric chloride ASTM G48-76 test which specifies a test solution of approximately 10% FeCl3. Several workers involved in MIC have proposed that this test be used to survey and rank stainless steels as a rapid method to determine MIC susceptibility. This article attempts to test the suitability of this extrapolation and presents data from the corrosion of two 6% and one 2.5% molybdenum stainless steel alloys under MIC and ferric chloride attack.

Relatively non-destructive techniques were employed including open-circuit potential (OCP) measurements and electrochemical impedance spectroscopy (EIS). EIS was selected to obtain average corrosion rate data since the small amplitude perturbing signal appears to disturb the biofilm very little. Furthermore, the information obtained by EIS has the potential to provide mechanistic information unavailable by direct current methods.

EXPERIMENTAL PROCEDURE

Bacterial Cultures

Bacteria were isolated from the deposits associated with a MIC attacked admiralty brass tube. The characteristics of these organisms are listed in table 1. In general terms, elements such as nickel are toxic to bacteria. Thus the growth of bacteria involved in corrosion on a metal containing high quantities of nickel may be depressed by these corrosion products. Since two of the alloys tested contain high quantities of nickel, bacterial strains were isolated that were nickel "tolerant". This was achieved by isolation with media containing a ten-fold increase in nickel and copper as usually is present in the trace elements (7). This concentration exerts a significant selective pressure on the type of organisms isolated. Once isolated the organisms were identified by Minitek™, classical microbiological techniques (Gram stain etc) and by lipid identification/library comparison using the Hewlett-Packard Microbial ID system. Final decision upon the genus and species of each isolate was based upon consideration of the results from all three techniques.

Electrolyte

Bacterial Test Medium. This was essentially a "freshwater" electrolyte and contained (g/L) Na_2SO_4 1.0, KH_2PO_4 0.1, NH_4Cl 0.2, $MgCl_2.6H_2O$ 0.4, KCl 0.1, $CaCl_2.2H_2O$ 0.05, microcrystalline cellulose 0.5, starch 0.1, chitin 0.1, glucose 0.1, yeast extract 0.05, Na lactate 0.05. After cooling suitable complex vitamins and trace elements were added (7). The final pH was adjusted to 8.2. The medium was subsequently pumped via sterile tubing into glass reaction kettles (working volume 1800 ml) which had been previously sterilized by ethylene oxide gas. After inoculation the medium was stirred for approximately 1 minute each day. Otherwise "quiet" solution conditions were maintained.

Ferric Chloride Electrolyte. This was prepared as described by the G48-76 ASTM standard (8). Ferric chloride (AR grade) 100g was dissolved in 900 ml of distilled water and passed through a Whatman No.1 cellulose filter. After 1800 ml were delivered to each test vessel, the exposure was accompanied with constant sparging with air for the duration of the experiment. The final pH of the solution was approximately 2.0. Total coupon surface area exposed per milliliter of electrolyte did not exceed 0.0034 cm^2/ml.

Alloy composition

Three alloys were employed in this test, two of which are designated A and B while the third was AISI 316 stainless steel. The chemical composition in the three alloys is given in table 2 with their designations using the Unified Numbering System (UNS).

Coupon preparation

Coupons were cut from sheet or tube to areas less than 3.5 cm^2 each. The reverse side of the coupons had a solder-connection brass screw attached and subsequently were embedded in Epo-Qwik (Buheler) epoxy resin. After grinding to a uniform 600 grit finish the edges were sealed with Microshield resin. The coupon assembly was then screwed into a tapped brass sleave via an 'O'-ring located in the test vessel.

Electrochemical data acquisition.

Average corrosion rate data were provided using a Solartron 1255 frequency response analyser in conjunction with a EG & G PAR 275 potentiostat fitted with modulating circuit (option 92). All measurements were taken with a 5 mV amplitude signal between 10 KHz and 5 mHz at the open circuit potential. The data was retrieved using software from Scribner Associates and is presented as complex plane (imaginary Z" versus real Z' impedance) and Bode diagrams (log impedance vs. log frequency and phase angle vs. log frequency). Electrochemical impedance spectroscopy enables the examination of a corrosion system by the application of a series of sinusoidal perturbations in the potential over many frequencies

and observing the current that results. Impedance can be calculated as a function of frequency which in part describes not just the rate of corrosion but the mechanism(s) involved. For further discussions on the utility of EIS as applied to corrosion systems please see MacDonald, 1987, (11).

Open circuit potential (OCP) measurements were taken using a Solartron 7081 digital voltmeter connected via a Solatron 7010 scanner to all the working electrodes in the system under test. All potential measurements were made versus a saturated calomel electrode (SCE). Data was retrieved via an IEEE cable into a IBM-compatable 286 computer with a macro written in LOTUS MEASURE. Measurements were taken and stored every 10 minutes.

RESULTS

In figure 1 OCP data showed that the free potentials of the electrodes in contact with the bacterial consortium fluctuated significantly with time. Because data were not taken for the first 12 hours the "zero" time marker in figure 1 corresponds to 12 hours immersion in the electrolyte. Thus bacteria were entering early logarithmic phase of growth just as data collection began (ie. have initiated corrosion-influencing processes). The data show that in each alloy the OCP declines rapidly in the order of 170 mV for alloy A, 360 mV for alloy B, and 80 mV for 316.

These results indicate that the microorganisms are involved in two processes: consumption of oxygen and the onset of pitting. Separation of these two events by OCP alone is however quite difficult. While the initial pH of the medium was 8.2, production of acids by the microorganisms drove the pH down to approximately 4.5 as measured by pH meter.

Data from previous studies indicate that the initial OCP value for 316SS and possibly those for the other alloys would be at least a hundred millivolts more positive (+ noble). The 316 in particular exhibits a "recovery" movement of the OCP after approximately 800 mins (note in figure 1 the time increments are equivalent to ten mins). This swing in the positive (+) direction shows that the consumption of oxygen by the bacteria is decreasing and/or that the bacterially influenced propagation of pits is slowing or stopped.

Open circuit potential measurements in the first few hours of these alloys exposed to 10% ferric chloride show quite stable values several hundred millivolts more positive (+) than those exhibited by the alloys in contact with the bacteria. Alloy A, for example, was at approximately +0.21 V/SCE, Alloy B at +0.45 V/SCE and 316SS at -0.09 V/SCE. After a further 16 hour exposure the mean OCP for alloy A was +0.254 V/SCE, +0.396 V/SCE for alloy B, and -0.125 V/SCE for 316 stainless steel.

Average corrosion data obtained by electrochemical impedance spectroscopy (EIS) is displayed in three formats. In figure 3(i) the diagrams indicate that alloy A corroded very slowly with an

estimated charge transfer resistance (Rct) of 10^5 ohms.cm2. At this time the 316 stainless steel had an estimated Rct of 60 K.ohms.cm2. Alloy B however had a high frequency (10 KHz to 1 Hz) capacitive loop indicative of a charge transfer process with Rct of 5000 ohms.cm2. In the same diagram low frequency (1 Hz to 5 mHz) data gave an apparent incremental increase in imaginary impedance (Z") with increase in the real impedance (Z'). EIS spectra initially and after 45 hours showed that the corrosion rate in all three alloys was very slow (Rct > 50 K.ohms.cm2).

Ferric chloride testing in figure 3(ii) gave a very small capacitive loop associated with 316 stainless steel (Rct = 210 ohm.cm2), a significantly larger one for alloy A (Rct = 7500 ohms.cm2) and for alloy B (Rct = 70 K.ohms.cm2).

The above results are replotted in Bode format in figure 4. These clearly show the shoulder associated with the charge transfer process in alloy B (figure 4 i). In figure 4 (ii) the phase angle defines the frequency range where the charge transfer process in alloy B occurs. In figure 4 (iii) the corrosion rates of the alloys exposed to ferric chloride are very well separated: the ranking order being (best corrosion resistance - worst) B, A, 316SS. In addition the phase angle diagram (figure 4 iv) shows that the "chemical" corrosion processes trend to higher frequencies as the corrosion rate increases.

DISCUSSION

Stainless steels are exceptional structural materials, with a good balance of mechanical properties, fabrication characteristics, relatively good weldability and good corrosion resistance (4). While industry produces several extremely corrosive environments (extremes in pH, redox potential, salinity etc.) raw, untreated freshwater is not considered one of them. Consequently, appreciation of MIC on stainless steels under such conditions is rather sparse. The new 6% molybdenum alloys appear to provide excellent resistance against aggressive solutions usually found in the process industry (9). Conventional testing of such however, typically employs corrosive solutions such as hydrochloric and sulfuric acids, and 3% sodium and ferric chlorides. Thus the characterization of many new alloys depends upon their performance in purely "chemical" corrosion systems. This article compares corrosion data obtained from both microbiological as well as chemical corrosion systems.

The open circuit potentials obtained from exposure to bacteria in freshwater were very different from those obtained during an exposure to 10 % ferric chloride. This implies that these two test environments were very different and very different corrosion mechanisms were involved. An example of this is the difference in open circuit potential: in ferric chloride the potentials were several hundred millivolts higher in the "passive" region as

opposed to the bacterial solutions. The performance of an alloy in the so-called "passive" region is very different from that in its "active" region for example (10).

The average corrosion rate data obtained by EIS indicates that after approximately 30 hours exposure to the bacteria, the corrosion rate of alloy B was substantially faster than either A or 316 stainless steel. Before and after this time the corrosion rates of all the alloys were very slow (due no doubt to the slow growth of the organisms in "lag" and "stationary" growth phases. Thus at a particular time alloy B did not perform in the ranking of corrosion resistance predicted by the ferric chloride tests presented in this article. This indicates that accelerated chemical corrosion tests designed to mimic microbiologically influenced corrosion cannot be relied upon to behave consistently with actual alloy performance in the environment.

The impedance diagrams obtained for alloy B indicate that while the charge transfer process is observed at the higher frequencies (10 KHz - 1 Hz), some presumably diffusive processes are observed at the lower frequencies (1 Hz - 5 mHz). This contrasts radically with those diagrams obtained from the ferric chloride tests where a single capacitive loop was observed in all cases. This confirms previous studies (3) with stainless steels where EIS data showed a significant diffusive component in conjunction with a charge transfer process under MIC attack. Previous studies have also shown single capacitive loops associated with stainless steels in ferric chloride even though "pitting" is considered the main process as opposed to uniform corrosion (3).

The mechanism of microbiological attack of stainless steel is still obscure. This laboratory has observed the deterioration of several different stainless steels associated with MIC attack. We have consistently observed the lowering of the open circuit potential in conjunction with the acceleration of the corrosion rate (12). Several bacteria of the type described in this article consume oxygen which would contribute to this lowering of the OCP. The introduction of nickel and copper-tolerant bacteria into this test matrix may have involved the selective removal of nickel from the three alloys examined. Such a mechanism has been proposed by Stoecker, 1984 (13) for other alloys although no information is available to support such a hypothesis for the alloys tested here. This laboratory is currently investigating nickel-loss from high molybdenum alloys and the activity of microorganisms on their surfaces.

LITERATURE CITED

1. D.E. Nivens, P.D. Nichols, J.M. Henson, G.G. Geesey, and D.C. White. Reversible acceleration of the corrosion of AISI 304 stainless steel exposed to seawater induced by growth and secretions of the marine bacterium Vibrio natriegens. Corrosion, 41, 201-210. 1986.

2. R.E. Tatnall. Case histories: Bacteria induced corrosion. Corrosion 19(8), 41-48.

3. N.J.E. Dowling, M.J. Franklin, D.C. White, C.H. Lee, and C. Lundin. The effect of microbiologically influenced corrosion on stainless steel weldments in artificial seawater. Corrosion 89, April 17-21, 1989.

4. D. Peckner and I.M. Bernstein. Handbook of stainless steels. McGraw-Hill, N.Y. 1977.

5. G. Okamoto. Passive film of 18-8 stainless steel structure and its function. Corrosion Science 13, 471-489.

6. K.V.E. Maleczki and G. Horanyi. On the simultaneous role of Cr in the passivity of stainless steel and in the sorbtion of HSO4 and Cl- ions in the passive film. Electrochimica Acta 33, 1775-1778.

7. F. Widdel and N. Pfennig. Dissimilatory suphate- or sulphur-reducing bacteria. In: Bergey's manual of systematic bacteriology. Vol.1. Ed. Krieg N. Williams and Wilkins, Baltimore, London.

8. ASTM. Annual book of ASTM standards. Section 3: Metals Test Methods and Analytical Procedures. Volume 03.02: Wear and Erosion; Metal Corrosion. ASTM Philadelphia PA.

9. J.R. Kearns and H.E. Deverell. The use of nitrogen to improve the corrosion resistance of FeCrNiMo alloys for the chemical process industries. Materials Performance. 26(6), 18-28. 1987.

10. Z. Szllarska-Smialowska. Pitting corrosion of metals. NACE, Houston, Texas. 1986.

11. J.R. MacDonald. (1987). Impedance spectroscopy: Emphasizing solid state materials and systems.

12. X. Zhang, R.A. Buchanan, E.E. Stansbury, and N.J.E. Dowling (1989). Electrochemical responses of structural materials to microbially influenced corrosion. Article # 512. Corrosion '89. New Orleans.

13. J.G. Stoecker (1984). Guide for the investigation of microbiologically induced corrosion. Materials Performance. 23, August. 48-55

TABLE 1: Distribution of microorganisms used in exposure study.

MIS Identification	Oxidase	Catalase	Slime	Acid	Ni/Cu resistant	
Bacillus megaterium	-	+	3+	slt.		(from FeOx enrichment)
Bacillus thuringiensis	-	-	-	1+		(from FeRed enrichment)
Pseudomonas picketti	+	-	slt.	-		
Bacillus sp.	-	-	-	1+	+	
Bacillus sp.	-	+	-	1+	+	
Bacillus pumilus	-	+	-	1+	+	
Bacillus brevis	-	+	-	1+	+	
Bacillus mycoides	-	+	-	2+		
Bacillus megaterium #2	-	+	1+	2+	+	

Sulfate reducer - (vibroid and growth on lactate)

TABLE 2: Chemical composition by weight percentage in the three metals under test.

Element	A UNS S31254	B UNS NO8367	316SS UNS 31600
Cr	20.0	20.0	17.0
Ni	18.0	24.0	12.0
Cu	0.7	0.15	0.18
Mo	6.1	6.5	2.11
C	0.02	0.03	0.08
N	0.2	0.2	0.05
S	0.01	0.002	0.011
P	0.03	0.025	0.024
Si	0.8	0.4	0.47
Mn	0.9	0.5	1.66

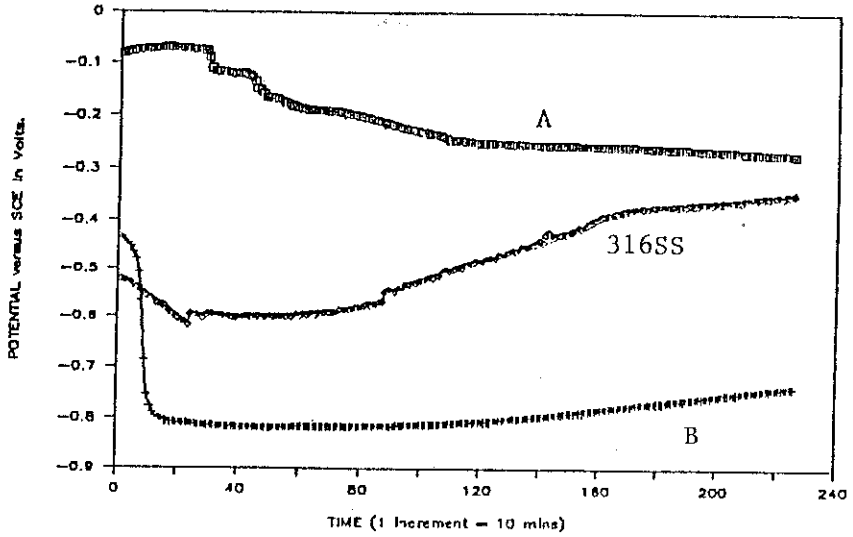

Figure 1: OCP data from the exposure of alloys A,B and AISI 316 to bacterial corrosion.

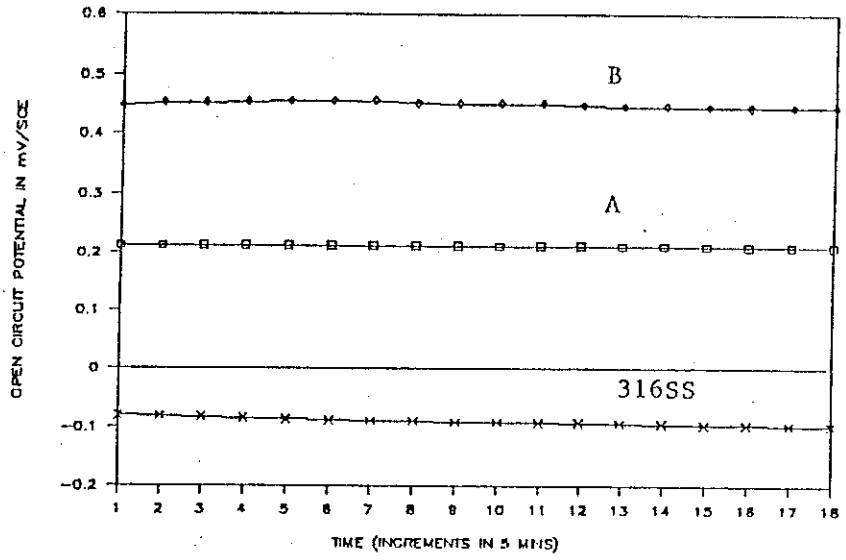

Figure 2: OCP data from the exposure of alloys A,B, and AISI 316 to ferric chloride attack.

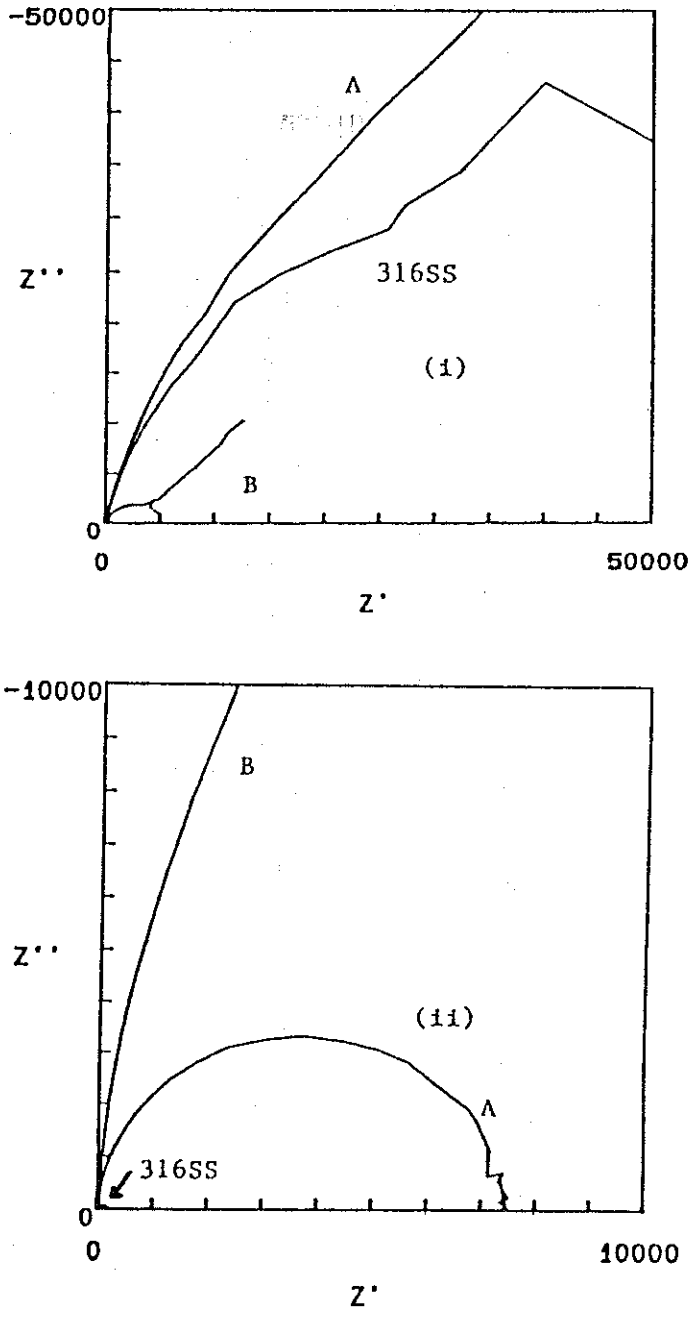

Figure 3: Complex plane diagram of the impedance data obtained from the three stainless steel alloys after approximately 30 hours exposure to bacterial corrosion (i) and 1-5 hours exposure to ferric chloride (ii).

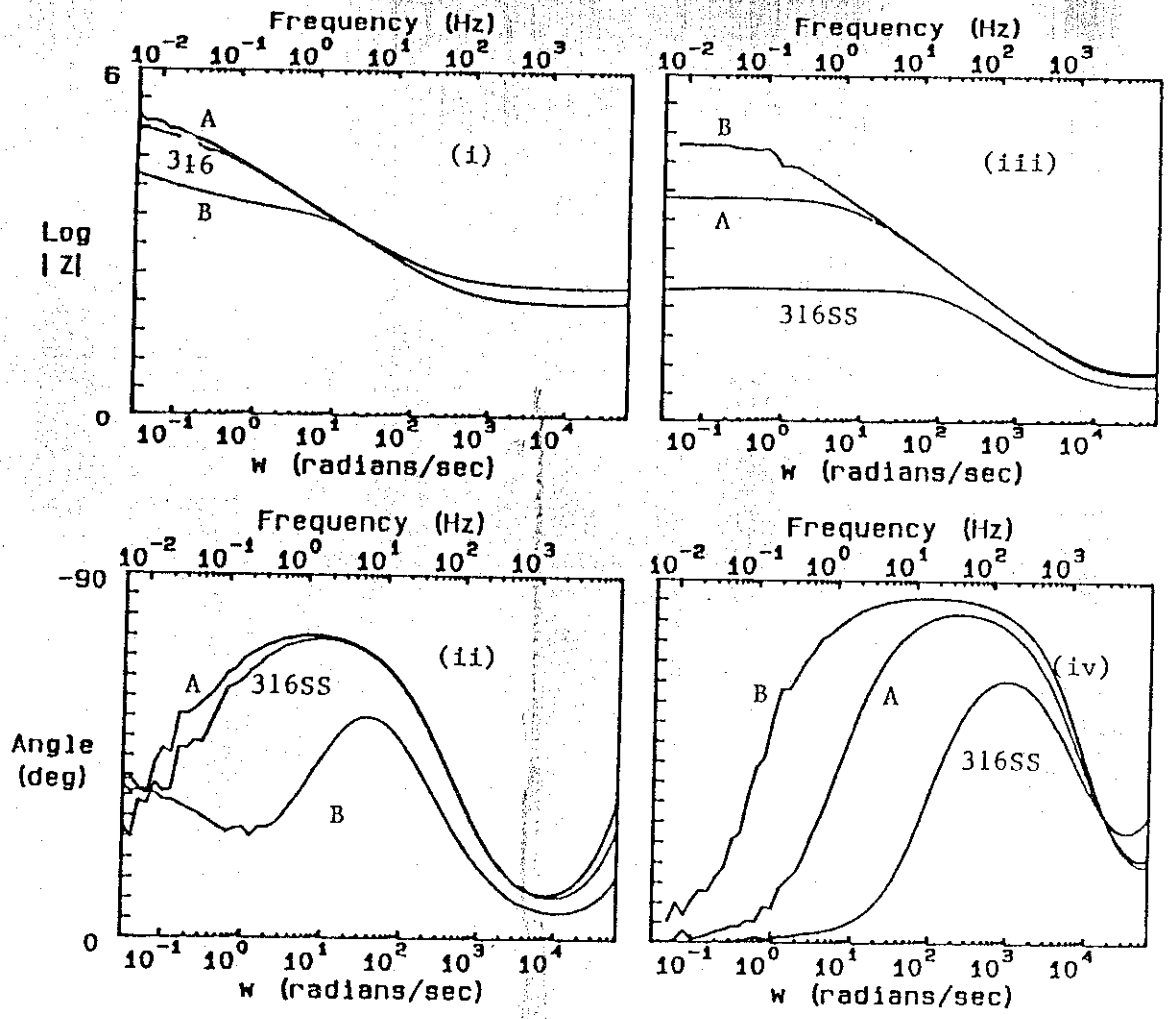

Figure 4: Bode diagrams of the impedance data obtained from the three stainless steels after approximately 30 hours exposure to bacterial corrosion (i,ii) and 1-5 hours exposure to ferric chloride (iii, iv).